



図3 大量ガンマグロブリン静注療法前後の臨床像
 a：大量ガンマグロブリン静注療法前(入院73日目)
 b：大量ガンマグロブリン静注療法後(入院81日目)。73日目(前)に比べ81日目(後)には顔面も急速に上皮化が進んでいる

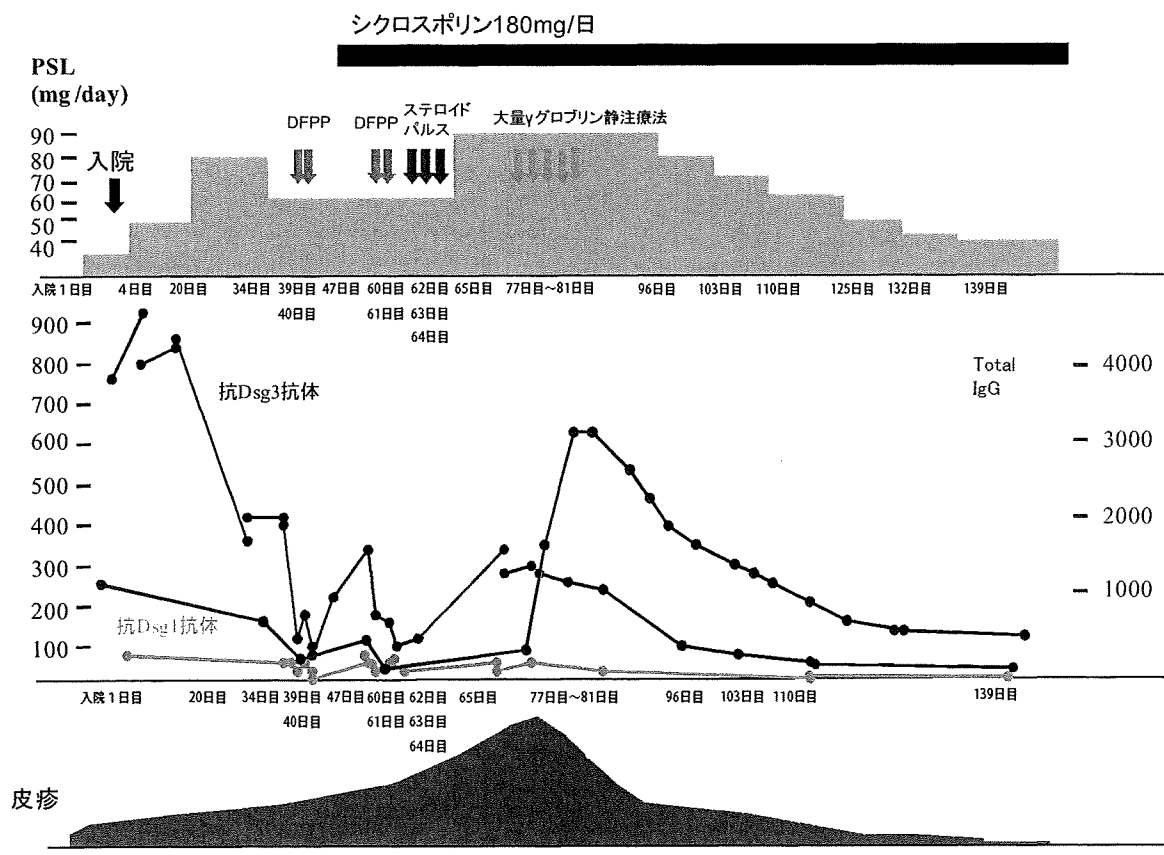


図4 治療と経過

mg/kg/日×5日間投与群が、プラセボ投与群に比較しプロトコル・オフまでの日数が有意に長く、大量ガンマグロブリン静注療法の有効性が確認された。(プロトコル・オフとは臨床症状の不変または悪化によりステロイド剤の増量、種類の変更、または他の追加治療を実施せざる

を得ないと判断した日時である。)このような臨床試験の結果をもとに、2008年10月より、献血グロバニン®-I-ニチャク 400 mg/kg/日×5日間が尋常性天疱瘡に対して保険適用になった。従来の治療に抵抗性の尋常性天疱瘡の患者に効果的で、安全な治療法と考えられる。

本症例は、長期大量ステロイド内服、血漿交換療法、シクロスポリン内服療法、ステロイドパルス療法を行い、PSL 90 mg/日に増量しても皮疹は軽快せず、抗 Dsg3 抗体価も低下しない、非常に難治な症例であった。しかし、大量ガンマグロブリン静注療法開始後、数日で皮疹の改善が見られた。ガンマグロブリン投与中に 37.6 度の発熱を 1 日認めたが、特に治療せず軽快した。その後抗 Dsg3 抗体価も徐々に低下したため、大量ガンマグロブリン静注療法が奏効したと考えた。

また、本症例は極めて抗体産生が強いため、DFPP 後にシクロスポリン内服療法、ステロイドパルス療法、PSL 90 mg/日内服を併用せざるを得なかった。しかし DFPP 後の低ガンマグロブリン血症時に、強い免疫抑制療法を加えるのは、日和見感染のリスクが高まるため、そのリスクを少しでも下げる意味においても大量ガンマグロブリン静注療法は選択肢として有用であると考えられる。さらに Aoyama ら²²⁾ が報告しているように、DFPP 後のリバウンド対策としても大量ガンマグロブリン静注療法は有用な治療法であると考えた。

大量ガンマグロブリン静注療法のメカニズムは、さまざまな仮説が言われているがいまだ不明である。大量にガンマグロブリンを投与することによって、ガンマグロブリンの異化が亢進し、抗 Dsg3 抗体も分解されるという考えもある¹⁰⁾。本症例も、総 IgG 量の低下とともに、すみやかに抗 Dsg3 抗体価も低下した。しかし、本症例のもう一つの特徴として、大量ガンマグロブリン静注療法直後に上皮化などの明らかな改善がみられており、抗 Dsg3 抗体価の減少とは別個の作用機序が存在することも考えられる。今後さらなる症例の蓄積が、治療効果の判定やメカニズムの解明において必要であろう。

本論文の要旨の一部は第 30 回水疱症研究会(2008 年 10 月, 東京), 第 49 回愛媛地方会(2009 年 3 月 1 日, 愛媛), 第 108 回日本皮膚科学会総会(2009 年 4 月, 福岡市)において報告した。

文 献

- 1) Stanley JR, Amagai M: Pemphigus, bullous impetigo, and the staphylococcal scalded-skin syndrome. *New Engl J Med* 355: 1800-1810, 2006.
- 2) Harman KE, Albert S, Black MM: Guidelines for the management of pemphigus vulgaris. *Br J Dermatol* 149: 926-937, 2003.
- 3) Ikeda S et al: History of the establishment and revision of diagnostic criteria, severity index and therapeutic guidelines for pemphigus in Japan. *Arch Dermatol Res* 295: S12-S16, 2003.
- 4) Chams-Davatchi C et al: Randomized controlled open-label trial of four treatment regimens for pemphigus vulgaris. *J Am Acad Dermatol* 57: 622-628, 2007.
- 5) Hashimoto T: Treatment strategies for pemphigus vulgaris in Japan: expert opin. *Pharmacother* 9: 1519-1530, 2008.
- 6) Tappeiner G, Steiner A: High-dosage intravenous gamma globulin: Therapeutic failure in pemphigus and pemphigoid. *J Am Acad Dermatol* 20: 684-685, 1989.
- 7) Segura S et al: High-dose intravenous immunoglobulins for the treatment of autoimmune mucocutaneous blistering diseases: Evaluation of its use in 19 cases. *J Am Acad Dermatol* 56: 960-967, 2007.
- 8) Ahmed AR et al: Treatment of pemphigus vulgaris with rituximab and intravenous immune globulin. *New Engl J Med* 355: 1772-1779, 2006.
- 9) Sami N et al: Corticosteroid-sparing effect of intravenous immunoglobulin therapy in patients with pemphigus vulgaris. *Arch Dermatol* 138: 1158-1162, 2002.
- 10) Bystryń JC, Jiao D, Natow S: Treatment of pemphigus with intravenous immunoglobulin. *J Am Acad Dermatol* 47: 358-363, 2002.
- 11) Ahmed AR: Intravenous immunoglobulin therapy in the treatment of patients with pemphigus vulgaris unresponsive to conventional immunosuppressive treatment. *J Am Acad Dermatol* 45: 679-690, 2001.
- 12) Ahmed AR, Dahl MV: Consensus statement on the use of intravenous immunoglobulin therapy in the treatment of autoimmune mucocutaneous blistering diseases. *Arch Dermatol* 139: 1051-1059, 2003.
- 13) Beckers RC et al: Adjuvant high-dose intravenous gammaglobulin in the treatment of pemphigus and bullous pemphigoid: experience in six patients. *Br J Dermatol* 133: 289-293, 1995.
- 14) Harman KE, Black MM: High-dose intravenous immune globulin for the treatment of autoimmune blistering diseases: an evaluation of its use in 14 cases. *Br J Dermatol* 140: 865-874, 1999.
- 15) Mignogna MD et al: Adjuvant high-dose intravenous immunoglobulin therapy can be easily and safely introduced as an alternative treatment in patients with severe pemphigus vulgaris. *Am J Clin Dermatol* 9: 323-331, 2008.
- 16) Baum S et al: The role of IVIg treatment in severe pemphigus vulgaris. *JEADV* 20: 548-552, 2006.
- 17) Czernik A, Beutner EH, Bystryń JC: Intravenous immunoglobulin selectively decreases circulating autoantibodies in pemphigus. *J Am Acad Dermatol* 58: 796-801, 2008.
- 18) 木村 淳: CIDP, MMN に対する献血グロベニン-I-ニチヤクの使用成績調査結果. *診療と新薬* 40: 297-316, 2003.
- 19) 日本製薬株式会社: 川崎病における献血グロベニン-I-ニチヤクの使用成績調査結果. *診療と新薬* 44: 845-870, 2007.
- 20) Saito E et al: Efficacy of high-dose intravenous immunoglobulin therapy in Japanese patients with steroid-resistant polymyositis and dermatomyositis. *Mod Rheumatol* 18: 34-44, 2008.
- 21) Zandman-Goddard G, Levy Y, Shoenfeld Y: Intravenous immunoglobulin therapy and systemic lupus erythematosus. *Clin Rev Allergy Immunol* 29: 219-228, 2005.
- 22) Aoyama Y et al: Severe pemphigus vulgaris: successful combination therapy of plasmapheresis followed by intravenous high-dose immunoglobulin to prevent rebound increase in pathogenic IgG. *Eur J Dermatol* 18: 557-560, 2008.
- 23) Amagai M et al: A randomized double-blind trial of intravenous immunoglobulin for pemphigus. *J Am Acad Dermatol* (J Am Acad Dermatol 60: 595-603, 2009.)
(2009 年 3 月 17 日 受付・2009 年 5 月 14 日 採用決定)

別刷請求先: 〒791-0295 東温市志津川
愛媛大学大学院医学系研究科
感覚皮膚医学
石川真奈美

Successful Treatment of Severe Intractable Pemphigus Vulgaris with High-dose Intravenous Immunoglobulin

Manami ISHIKAWA, Yuji SHIRAKATA, Shinji MURAKAMI, Mikiko TOHYAMA,
Keiko TANIMOTO, Yukari URABE, Naoki SATO, Saori MIYAWAKI,
Hidenori OKAZAKI, Satoshi HIRAKAWA, Sho TOKUMARU, Yasushi HANAKAWA,
Koji SAYAMA and Koji HASHIMOTO

Department of Dermatology, Ehime University Graduate School of Medicine
Toon 791-0295, Japan (Director: Prof. K. Hashimoto)

We report a case of a 46-year-old Japanese female with severe pemphigus vulgaris successfully treated with high-dose intravenous immunoglobulin. Oral high-dose corticosteroids and double-filtration plasmapheresis (DFPP) was unsuccessful in suppressing her disease activity. Addition of cyclosporine and DFPP, immediately followed by pulse therapy with intravenous (IV) methylprednisolone (1,000 mg/day for 3 days), was only partially successful. We decided to use intravenous immunoglobulin (IVIG; 400 mg/kg/day for 5 days). After IVIG therapy, erosions began to heal rapidly, and the bullae completely disappeared, along with a decrease in anti-Dsg3 antibody titer.

薬剤性過敏症症候群 (DIHS) の特徴的な顔面の所見と HHV-6 再活性化との 時間的關係

岡崎 秀規 藤山 幹子 村上 信司 石川真奈美
佐藤 直樹 宮脇さおり 白石 研 橋本 公二

要 旨

2001年から2007年の間に当科で経験したDIHS症例のうち、DIHSの顔面の特徴的皮疹を示し、HHV-6の再活性化の時期を特定することのできた6例について、両者の時間的關係を検討した。6例全例で顔面の特徴的皮疹の出現がHHV-6再活性化に先行していることが確認された。

DIHSの顔面の特徴的皮疹は、DIHSの診断の手助けになるとともに、HHV-6の再活性化と、それによる症状の再燃を予測する重要な手がかりになると考えられた。

はじめに

drug-induced hypersensitivity syndrome (DIHS) は発熱、リンパ節腫脹、肝機能障害、血液異常を伴う重症薬疹の一型で、ヒトヘルペスウイルス6 (HHV-6) の再活性化と臨床症状の再燃が見られる。皮疹は紅斑丘疹型、多形紅斑型であるが、顔面にDIHSに特徴的とされる皮膚症状、すなわち顔面の紅斑、浮腫、口囲の紅色丘疹、膿疱、小水疱、鱗屑がみられることがある。今回我々はDIHSの顔面の特徴的皮疹とHHV-6再活性化の時間的關係を検討した。

症 例

2001年から2007年の間に当科で経験した血清中のHHV-6 DNAの検出、あるいは全血中のHHV-6の増加により、再活性化の時期がほぼ特定できるDIHS症例6例について検討した。以下、症例1の経過を詳細に、症例2～6については概略を述べる。

症例1：44歳、男性。

既往歴：自律神経失調症。

現病歴：平成16年6月16日よりテグレート[®]、コントミン[®]内服開始。7月10日頃より全身倦怠感、背部の紅斑が出現。7月15日頃より頭部、上肢に紅斑が拡大し、掻痒感をみとめた。7月18日には39℃の発熱があり、当院救急外来受診、同日当科入院となった。

内服歴として平成14年8月20日からバキシル[®]、デパス[®]、ランドセン[®]、ソラナックス[®]。平成14年10月1日からカマグ[®]、平成16年6月16日からテグレート[®]、コントミン[®] (コントミン[®]は頓服で処方されており、数回服用したのみ) であり、これらの薬剤の中でも1カ月前より内服開始していたテグレート[®]、コントミン[®]を原因として疑った。全薬剤は入院日7月18日より中止した。

入院時臨床像 (図1)：被髪頭部、顔面には紅斑、赤色丘疹が多発、癒合し、顔面、耳介には浮腫を認めた。眼周囲には紅斑を認めなかった。また鼻孔周囲、外耳道には軽度の紅斑を認めた。四肢体幹には毛孔一致性の丘疹が多発、癒合していた。眼球、眼瞼結膜は異常なく、口腔内では口蓋に2mm大の紅斑と、舌の側縁には直径2mm大の浅いアフタを認めた。また右後頸部リンパ節は腫脹していた。

臨床検査所見 (入院3日目)：末梢血；WBC 22,400/ μ l (stab 16.5%, seg 48.0%, lymph 5.5%, mono 4.5%, eosino 25.5%, baso 0.0%, atypical lymph 0.0%), RBC 5.80×10^3 / μ l, Hb 16.9g/dl, Ht 50.4%, PLT 25.5×10^4 / μ l。血液生化学；T.bil 0.5mg/dl, D.bil 0.1mg/dl, GOT 49IU/l, GPT 175IU/l, γ -GTP 490IU/l, LDH 577IU/l, ChE 143IU/l, ALP 466IU/l, LAP 125IU/l, AMY 83IU/l, CRP 6.21mg/dl, TP 5.9g/dl, Alb 3.2g/dl, Glo 2.5g/dl, BUN 7mg/dl, Cre 0.7mg/dl, Na 140mEq/l, K 4.1mEq/l, Cl 103mEq/l, IgG 842mg/dl, IgA 132mg/dl, IgM 21mg/dl, IgE 30IU/ml, T細胞分画；CD4 31%, CD8 42%。胸部X線と心電図に異常はみられな

愛媛大学大学院医学系研究科感覚皮膚医学 (主任：橋本公二教授)

平成21年2月12日受付、平成21年4月2日掲載決定
別刷請求先：(〒791-0295)愛媛県東温市志津川 愛媛大学大学院医学系研究科感覚皮膚医学 岡崎 秀規

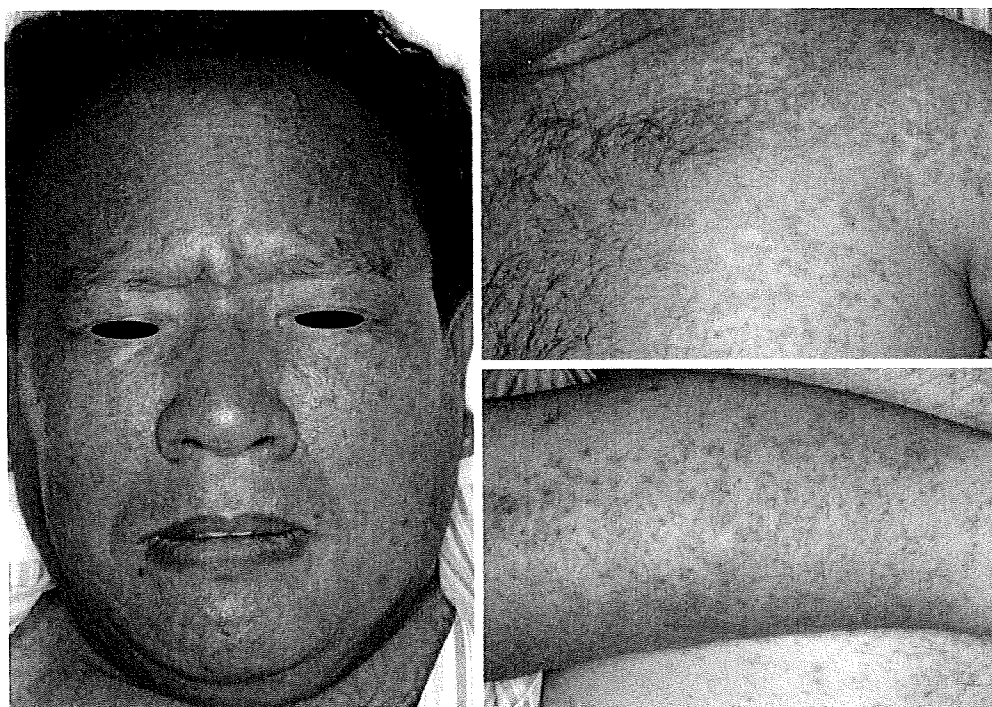


図1 初診時臨床像

頭部、口囲を含む顔面には赤色丘疹が多発、癒合し、顔面、耳介には浮腫を認めた。眼周囲には紅斑を認めなかった。四肢体幹には毛孔一致性の赤色丘疹が多発、癒合していた。

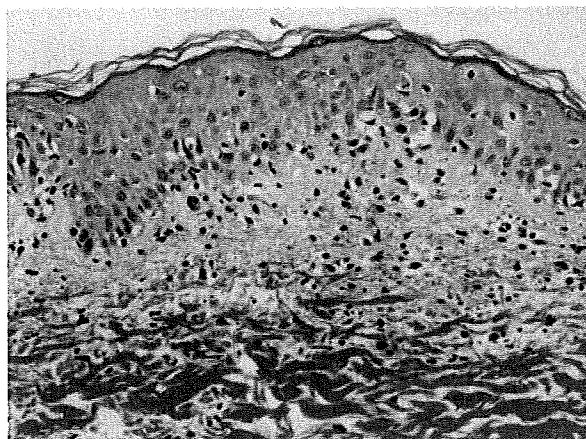


図2 病理組織像(強拡大)

表皮では液状変性、少数の個細胞壊死を、真皮上層ではリンパ球の浸潤を認めた。好酸球浸潤は認めなかった。

かった。

組織所見(図2)：背部の丘疹に対して皮膚生検を施行した。表皮角化細胞の少数の個細胞壊死と液状変性、真皮上層から中層にかけてのリンパ球の浸潤を認めた。組織学的には苔癬型組織反応であった。

経過(図3)：入院日(7月18日)からプレドニゾン(PSL)40mg/日の内服を開始したが依然37~38℃台の発熱を認め、顔面、頸部の浮腫は徐々に増悪し、息苦しさ(SpO₂98%)を訴えた(図4a)。耳鼻科受診したところ喉頭ファイバーの所見では喉頭左側に浮腫を認め、浮腫のさらなる増悪がみられれば気管切開も必要となるとのことであった。そこで21日よりPSLを80mg/日(0.8mg/kg)に増量したところ、解熱するとともに、顔面と頸部の浮腫、息苦しさ、全身の皮疹も徐々に軽快した(図4b)。しかし26日朝より39℃台の発熱と肝機能異常の増悪を認めた。血液中に多量のHHV-6 DNAが確認され、PSLを漸減した。発熱は2日間で解熱し、肝機能異常も28日をピークに正常化していった。このときに皮疹の明らかな再燃はなかったが、8月8日から手背、足背に赤色丘疹の新生を認めた。PSL内服は8月24日で中止し、皮疹は完全に消退した。全経過は約7週間であった。

ウイルス検査：HHV-6DNA copy数は、血清中では7月23日から検出(3,300copies/ml)され、26日には240万copies/mlにまで増加した後、経過とともに低下した。HHV-6 IgG抗体価は7月26日までは80倍であっ

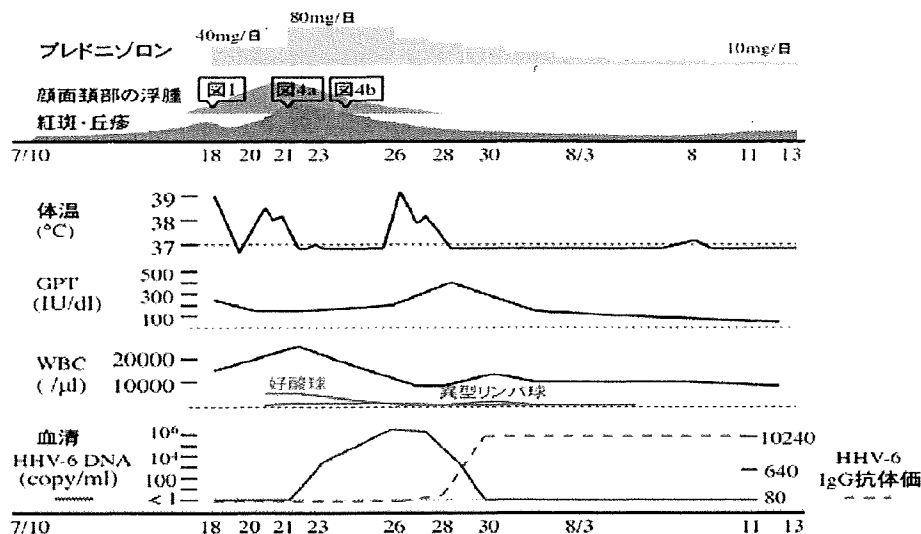


図3 臨床経過および血液所見の推移

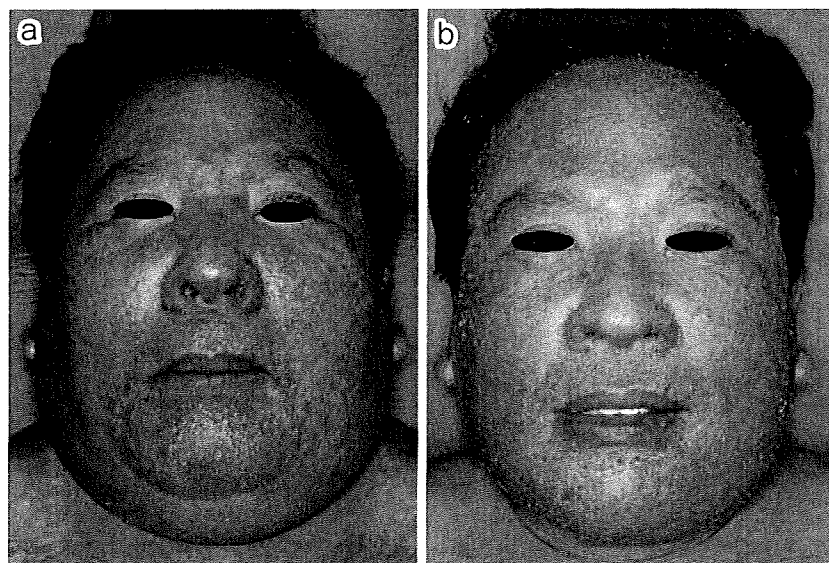


図4 顔面の臨床像

a: 7月21日 (第12病日): 全身の皮疹, 顔面の浮腫が著明であった. 喉頭の浮腫のため軽度の呼吸困難を生じていた. 鼻孔には紅斑を認める. 口囲には赤色丘疹が多発し, 膿疱, 痂皮, 鱗屑の付着も認める.
 b: 7月24日 (第15病日): 解熱しており, 顔面の腫脹は軽快傾向. 全身の紅斑も褐色調を呈してきている. 口囲には多量の痂皮・鱗屑の付着を認める.

たが, 28日には320倍, 30日には10,240倍まで上昇した.

薬剤によるリンパ球刺激試験 (DLST): 原因薬剤と考えられるテグレトール®, コントミン®で施行した. 第11病日 (7月20日) のDLSTではテグレトール®,

コントミン®の stimulation index (SI.) はそれぞれ139%, 134%と共に陰性であったが, 第48病日 (8月26日) ではそれぞれ315%, 88%であり, テグレトール®で陽性であった. これによりテグレトール®が原因薬剤であると考えた.

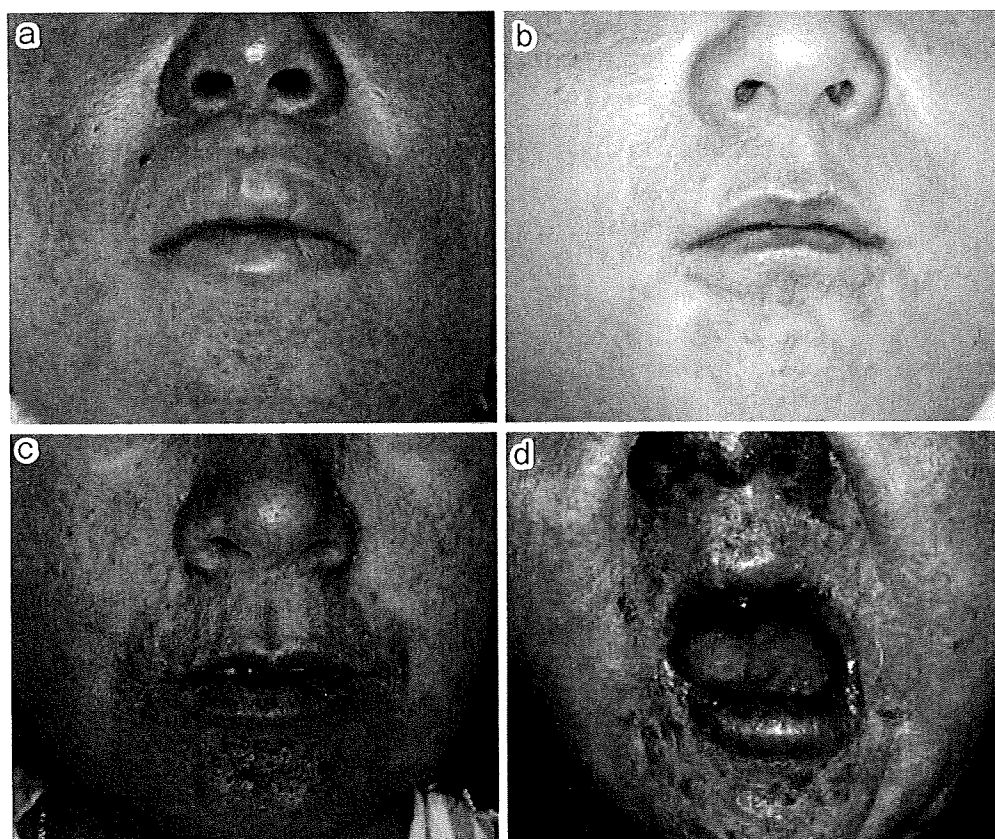


図5 DIHS4例の顔面の特徴的皮疹

程度は異なるものの、口囲の赤色丘疹、鱗屑、痂皮の付着、鼻孔の紅斑、顔面の浮腫を認める。

症例2：33歳，女性．エクセグラン[®]内服開始後15日経過して皮疹出現，その10日後にはフェノバール[®]内服に変更され皮疹は軽快したが，薬剤変更後7日経過して皮疹，発熱が出現．臨床症状再燃後3日目（第4病日）に当科初診，入院．初診時には顔面，頸部の強い浮腫と鼻孔周囲の紅斑，口囲の少数の赤色丘疹（図5a）を認めていた（患者持参の第3病日の写真では，口囲の皮疹は認めなかった）．第17病日にはじめて全血中にHHV-6DNAが出現した（200copies/ μ gDNA）が，血清中には検出されず，抗HHV-6IgG抗体価の上昇は伴わなかった．また発熱や臓器障害の再燃はなく皮疹の軽度の再燃を認めたのみであった．

症例3：12歳，男性．テグレトール[®]内服開始後23日目に発熱，顔面の紅斑が出現．第2病日の当科初診時には頬に淡い紅斑を認めるのみであったが，PSLの内服にも関わらず第8病日には口囲の紅色丘疹が確認された（図5b）．その後臨床的，血液学的に軽快傾向にあったが，第12病日から肝障害が再燃し，第15病

日からは39度台の発熱と皮疹が再燃した．同日の全血中でHHV-6DNAの出現（4,500copies/ μ gDNA）が確認されたが，血清中には検出されなかった．

症例4：66歳，男性．テグレトール[®]内服開始後37日目に皮疹出現．第11病日に当科初診，入院．第12病日には口囲の赤色丘疹が確認され第18病日に全血中にHHV-6DNA（380copies/ μ gDNA）が出現してきた．第21病日には皮疹の再燃と肝機能異常の増悪を認め，同日の血清，全血中でHHV-6DNAが確認された．

症例5：48歳，女性．アレビアチン[®]内服開始後2年経過して発症．発熱を自覚しその2日後より皮疹が出現．皮疹は顔面からはじまり拡大した．第16病日の当科初診時には顔面の特徴的皮疹を認め（図5c），第20病日には全血中に1,200copies/ μ gDNAのHHV-6DNAが検出され，第21病日には血清中にも検出された．発症から続いていた発熱はHHV-6DNAが血清から消失するとともに解熱し，血液学的に肝障害の再燃が認められた．

表 1 DIHS 症例の顔面の特徴的皮疹と HHV-6 再活性化のまとめ

症例	顔面の特徴的皮疹が確認された病日	HHV-6 再活性化を認めた病日
1	11	14 (血清)
2	4	17 (全血)
3	8	15 (全血)
4	12	18 (全血)
5	16 (初診日)	20 (全血)
6	12 (初診日)	19 (血清)

症例 6 : 48 歳, 女性. カルバマゼピン[®], フェノバル[®]内服開始から約 2 年経過して発症した. 第 12 病日の当科初診時には顔面の特徴的皮疹が認められた (図 5d). ステロイド剤の全身投与により解熱し, 全身状態も改善していたが, 第 19 病日には血清, 全血より HHV-6DNA (39,000copies/ml, 71,000copies/ μ gDNA) が検出された. 第 23 病日には発熱の再燃がみられ, 続いて皮疹の再燃が, 血液学的には肝障害の再燃が認められた.

症例 1 は, 顔面と頸部の浮腫が非常に強く呼吸苦を伴ったことが特異であった. 顔面では浮腫とともに鼻孔, 外耳道の紅斑, 口囲の赤色丘疹, 鱗屑, 痂皮の付着がみられており (図 4a), いわゆる DIHS に特徴的な顔面の所見と考えた. この顔面の特徴的な皮疹は 7 月 20 日 (第 11 病日) に確認されたが, その 3 日後 (第 14 病日) には血清中に HHV-6 DNA が検出された. つまり, 顔面浮腫と特徴的皮疹は, HHV-6 の再活性化に 3 日先行して認められたということになる.

症例 2~6 についても程度は異なるものの, 口囲の赤色丘疹, 鱗屑, 痂皮の付着, 鼻孔周囲の紅斑, 顔面の浮腫を認めた. 皮疹出現日を特定できた 3 例 (症例 2~4) では, いずれも特徴的皮疹出現後に HHV-6 の再活性化を認めており, その間の日数はそれぞれ 13, 7, 6 日であった. 症例 5, 6 においては, 初診時には既に顔面の特徴的皮疹が確認されていたが, その時点では血液中の HHV-6 DNA は検出されず, それぞれ 4, 7 日経過して HHV-6 の再活性化が確認された. 以上を表 1 にまとめた.

考 察

DIHS の特徴的な皮疹は, 厚生労働省研究班の診断基準の参考所見において「顔面の浮腫, 口囲の紅色丘疹, 膿疱, 小水疱, 鱗屑は特徴的である」と記載されている¹⁾. この顔面の皮疹については以前より知られて

おり, 1996 年に Callot らの論文²⁾に顔面頸部の浮腫, 小水疱, 膿疱が Hypersensitivity Syndrome の顔面にみられる所見として記されている. また Drug Rash with Eosinophilia and Systemic Symptoms (DRESS) の疾患概念が提唱されてからは, DRESS では顔面の浮腫と皮疹があることが特徴であると記載されている^{3) 4)}, 以上のようにこの顔面の所見は国内外を問わず共通している.

初診時より顔面の特徴的皮疹を認めた症例 5, 6 についてはその 4, 7 日後に HHV-6 の再活性化を確認し, 症例 1~4 における特徴的皮疹の確認から, HHV-6 の増加を認めるまでの期間は 3, 13, 7, 6 日であった. 症例 2 は特徴的皮疹出現から HHV-6 再活性化までの期間が 13 日と最も長かった. この症例は HHV-6 抗体価の上昇を伴わず, また, HHV-6 再活性化による症状の再燃もみられなかったことより, 全血中の HHV-6 DNA の検討がなされていなければ非典型 DIHS の診断となる. この症例を除けば, 皮疹を確認した 1 週間前後で HHV-6 が再活性化している.

DIHS では, HHV-6 の再活性化に伴い, 臨床症状, 血液学的異常が再燃することがある. 最も多くみられるのは発熱と肝障害である⁵⁾. この症状の再燃は, 特別な治療を要さず軽快することが多い. 当科の 6 症例においては 5 例に肝障害の再燃が, 4 例に発熱の再燃がみられたが, いずれもステロイド薬を増量することなく, 数日で軽快した. しかし一度軽快したと思えたところに再燃する発熱や肝障害は, 本人や家族に不安を抱かせる. また, DIHS における HHV-6 の再活性化によると思われる脳炎・中枢神経障害^{6) 7)}や劇症 1 型糖尿病⁸⁾のような重症の病態の発症も報告されている. 顔面の特徴的な皮疹を認めた時点で, 今後の見通しを説明することができれば, 再燃を生じたときの不安を軽減させることが可能である. また, 治療する側においても, HHV-6 の再活性化を予想することで, 重症な病態の発生にも注意を払うことが可能である.

以上のように, 我々は, DIHS における特徴的な顔面の皮疹の出現時期と HHV-6 の再活性化の時期をウイルス DNA の定量という方法を用いて詳細に検討することにより, 前者が後者に先行することを明らかにした.

顔面の皮疹の発症機序は現時点では不明であるが, 今回の HHV-6 の再活性化が血液中における HHV-6 の出現の確認, すなわち HHV-6 ウイルス血症, によると定義していることを考慮すると, 次のような可能性

が考えられる。HHV-6 はどこかの組織でまず再活性化し、続いて血液中で活性化 T 細胞に感染し、全身の HHV-6 再活性化にいたると想定されている。従って、薬剤アレルギーに続いて、まず顔面で HHV-6 の再活性化がおき、血液中に拡大するということが考えられる。この仮説は、特徴的な顔面の皮疹が HHV-6 の再活性化に先行する時間的關係を説明するには極めて魅力的なものである。しかし、顔面の皮疹と HHV-6 の再活性化が全く関係ない可能性も否定できない。DIHS でみられるような顔面の浮腫は臨床的に acute generalized exanthematous pustulosis や Stevens-Johnson syndrome などの重症型薬疹などでもみとめられるこ

とがあり、鼻翼周囲や口囲の皮疹は軽度の場合には脂漏性皮膚炎に類似している。しかしこれらの疾患では一般的に HHV-6 の再活性化は検出されない。また HHV-6 の再活性化がよく経験される Graft-versus-host disease において DIHS でみられるような顔面の皮疹の出現を認めるといった報告もない。DIHS の顔面の皮疹と HHV-6 の再活性化の関連性を明らかにするためには、今後の症例の集積が必要である。

謝辞：本論文は厚生労働科学研究費補助金（難治性疾患克服研究事業）の援助を受けた。

文 献

- 1) 橋本公二：Stevens-Johnson 症候群，toxic epidermal necrosis (TEN) と hypersensitivity syndrome の診断基準および治療指針の研究，厚生科学特別研究事業 平成 17 年度総括研究報告，2005。
- 2) Callot V, Roujeau JC, Bagot M, et al: Drug-induced pseudolymphoma and hypersensitivity syndrome, *Arch Dermatol*, **132**: 1315-1321, 1996.
- 3) Revuz J, Valeyrie-Allanore L: Drug Reactions with Eosinophilia and systemic symptoms: Hypersensitivity Syndrome, In: Bologna JL, Jorizzo JL, Rapini RP (eds): *Dermatology*, 2nd Ed, Mosby Elsevier, Amsterdam, 2008, 310-311.
- 4) Descamps V, Valance A, Edlinger C, et al: Association of human herpesvirus 6 infection with drug reaction with eosinophilia and systemic symptoms, *Arch Dermatol*, **137**: 301-304, 2001.
- 5) Tohyama M, Hashimoto K, Yasukawa M, et al: Association of human herpesvirus 6 reactivation with the flaring and severity of drug-induced hypersensitivity syndrome, *Br J Dermatol*, **157**: 934-940, 2007.
- 6) Masaki T, Fukunaga A, Tohyama M, et al: Human herpes virus 6 encephalitis in allopurinol-induced hypersensitivity syndrome, *Acta Derm Venereol*, **83**: 128-131, 2003.
- 7) Fujino Y, Nakajima M, Inoue H, et al: Human herpesvirus 6 encephalitis associated with hypersensitivity syndrome, *Ann Neurol*, **51**: 771-774, 2002.
- 8) Sekine N, Motokura T, Oki T, et al: Rapid loss of insulin secretion in a patient with fulminant type 1 diabetes mellitus and carbanazepine hypersensitivity syndrome, *JAMA*, **285**: 1153-1154, 2001.

**The Relationship between the Appearance of the Characteristic Skin Eruption and HHV-6
Reactivation in Drug-induced Hypersensitivity Syndrome (DIHS)**

Hidenori Okazaki, Mikiko Tohyama, Shinji Murakami, Manami Ishikawa,
Naoki Satoh, Saori Miyawaki, Ken Shiraishi and Koji Hashimoto
Department of Dermatology, Ehime University Graduate School of Medicine

(Received February 12, 2009; accepted for publication April 2, 2009)

We studied the relationship between the appearance of the characteristic skin eruption and HHV-6 reactivation in DIHS. Six patients with DIHS, who were treated in Ehime University Hospital from 2001 to 2007, exhibited the characteristic skin eruption pattern that included erythema and edema in the face and perioral red papules, pustules, vesicles and scales. HHV-6 reactivation was observed in all six patients. The exact date of HHV-6 reactivation was confirmed by quantitative real-time polymerase chain reaction assay of serial serum or whole blood samples. In all DIHS six patients, the characteristic skin eruptions in the face always preceded HHV-6 reactivation. This is the first time that this characteristic sequential response has been elucidated.

(*Jpn J Dermatol* 119: 2187~2193, 2009)

Key words: drug-induced hypersensitivity syndrome (DIHS), facial characteristic skin eruption, HHV-6 reactivation

Tumor necrosis factor- α processing inhibitor-1 inhibits skin fibrosis in a bleomycin-induced murine model of scleroderma

Mika Terao, Hiroyuki Murota, Shun Kitaba and Ichiro Katayama

Department of Dermatology, Osaka University Graduate School of Medicine, Suita, Osaka, Japan

Correspondence: Hiroyuki Murota, Department of Dermatology, Osaka University Graduate School of Medicine, Box C5, 2-2 Yamadaoka, Suita, Osaka 565-0872, Japan, Tel: +81 6 6879 3031, Fax: +81 6 6879 3039, e-mail: h-murota@derma.med.osaka-u.ac.jp

Accepted for publication 14 July 2009

Abstract: Elevated serum concentration of soluble tumor necrosis factor receptor p55 (sTNFRp55) is known to correlate with the severity of systemic sclerosis (SSc). However, it has not been verified whether this increase contributes to the pathogenesis of SSc. In this study, we found that sTNFRp55 also is increased in the bleomycin (BLM)-induced murine model of SSc. Therefore, we examined the effect of tumor necrosis factor- α processing inhibitor-1 (TAPI-1), the inhibitor of TNFRp55 sheddase, in this model. TAPI-1 was administered weekly to mice with skin fibrosis induced by daily BLM injections. TAPI-1 significantly suppressed BLM-induced skin thickness and the number of

myofibroblasts. It also inhibited the increase of serum sTNFRp55 after 3 weeks of BLM injections. The mRNA expression of collagen type I α 1, transforming growth factor- β 1 and alpha smooth muscle actin were decreased by TAPI-1 administration. Taken together, these findings indicate that targeting the TNF α converting enzyme might be a new type of therapy for patients with SSc.

Key words: scleroderma – TAPI-1 – tumor necrosis factor- α – tumor necrosis factor- α converting enzyme – tumor necrosis factor receptor p55

Please cite this paper as: Tumor necrosis factor- α processing inhibitor-1 inhibits skin fibrosis in a bleomycin-induced murine model of scleroderma. *Experimental Dermatology* 2010; 19: 38–43.

Introduction

Systemic sclerosis (SSc) is a disease characterized by progressive fibrosis of multiple systems including the skin. Although a small number of studies have observed statistically significant benefits from immunomodulatory treatment, none of the major clinical trials using skin fibrosis as an endpoint have been clinically superior to placebo (1,2).

Skin fibrosis is caused by massive production of fibrous connective tissue in the dermis, which exceeds the rate of degradation (3). Transforming growth factor- β (TGF β), tumor necrosis factor- α (TNF α), various interferons and interleukins are known to induce or inhibit the expression of extracellular matrix genes or enzymes (4). One of the major cytokines involved in skin fibrosis is TGF β . It is the most potent inducer of connective tissue growth factor (CTGF), which promotes matrix deposition and fibroblast proliferation (4,5). Disruption of TGF β prevented the occurrence of fibrosis in 'tight skin' mice (6).

On the contrary, TNF α is known to have an antagonistic effect on TGF β by suppressing the induction of CTGF (7–9). We previously reported that wild-type mice with a disrupted TNF receptor p55 (TNFRp55) gene exhibited severe

skin fibrosis following bleomycin (BLM) treatment (10). The TNFRp55 $^{-/-}$ mice exhibited skin fibrosis starting on day 3 vs day 14 in wild-type mice. This result indicates that the TNFRp55 signalling pathway plays an important role in the mechanism of skin fibrosis induced by BLM.

Several previous studies have demonstrated the association of TNF α and TNFRp55 with the clinical symptoms of SSc patients. Expression of TNF α is detectable in the serum of patients at very early stages of SSc (11). The serum level of TNF α increases with the clinical severity and biological activity of the disease (12) and the serum level of soluble TNFRp55 (sTNFRp55) correlates with the severity of disease (13–15). sTNFRp55 is known to neutralize TNF α and inhibit its effects (13). Therefore, we assumed that an increase in sTNFRp55 (which results in TNF α neutralization and reduction of the TNFRp55 signalling) plays a key role in the pathomechanism of SSc.

In this study, we focussed on TNF α converting enzyme (TACE). TACE is a member of the disintegrin and metalloproteinase family that is responsible for the processing of pro-TNF α and TNF receptors (16,17). We hypothesized that TACE activity might be increased in SSc patients, which might result in an increase of serum TNF α and

sTNFRp55. We examined the effect of a TACE inhibitor (TNF- α processing inhibitor-1, TAPI-1) to see whether it has the ability to inhibit BLM-induced skin sclerosis in C57BL/6 mice. TAPI-1 significantly suppressed skin sclerosis induced by BLM and reduced fibrogenic cytokines. Therefore, it has the potential to be a new type of therapy for skin sclerosis in SSc patients.

Materials and methods

Cell culture

Isolation and culture of mouse keratinocytes and mouse fibroblasts were carried out as previously described (18,19). Full-thickness skin harvested from day 2 to day 4 newborn mice was treated with 4 mg/ml of dispase (Gibco; Invitrogen, Paisley, UK) for 1 h at 37°C. Next, the epidermis was peeled from the dermis. The epidermis was trypsinized to prepare single cells. It was then incubated in Human Keratinocyte Serum Free Medium (DS Pharma Biomedical, Osaka, Japan) for 6 h at 37°C under an atmosphere with 5% CO₂. This atmosphere allowed the cells to adhere in the culture dishes precoated with type-1 collagen (Asahi Techno Glass, Funabashi, Japan). Non-adherent cells were washed away with phosphate-buffered saline (PBS) twice, then cultured for 2–3 days in human keratinocyte serum-free medium before use in experiments.

The dermis was placed in PBS + 0.05% type-1 collagenase (Sigma-Aldrich, St Louis, MO, USA) and incubated at 37°C for 30 min with vigorous agitation to prepare single cells. After filtration, cells were centrifuged at 200 g for 10 min, resuspended in Dulbecco's Modified Eagle Medium (DMEM) + 10% Fetal Bovine Serum (FBS) and incubated at 37°C and 5% CO₂. Passage one or two fibroblasts were starved for 2 h and then used for experiments. For isolation of splenocytes, C57BL/6 mouse spleens were removed aseptically and passed through a sterile nylon 70 μ m cell strainer (BD bioscience, Bedford, MA, USA). The red blood cells were lysed by adding lysis buffer (0.15 M ammonium chloride) followed by centrifugation. The cell pellet was washed with PBS and cultured in RPMI-1640 medium containing 10% FBS. A mouse C3H muscle myoblast cell line (C2C12) was obtained from ECACC (Salisbury, UK), cultured in DMEM + 10% FBS and incubated at 37°C and 5% CO₂. Cells were starved overnight before the experiment.

BLM and TAPI-1 treatment

Six-week-old female C57BL/6 mice were obtained from Clea Japan (Osaka, Japan), Inc. Animal care was in accordance with the institutional guidelines of Osaka University. BLM (Nippon Kayaku, Tokyo, Japan) was dissolved in PBS at a concentration of 1 mg/ml. Daily injections of 100 μ l of BLM or PBS were administered subcutaneously to the shaved dorsal area for 3 weeks.

One micro mol of TAPI-1 (Biomol, Plymouth Meeting, PA, USA) was diluted in 25 μ l dimethyl sulfoxide (DMSO) and further diluted with 275 μ l of PBS and was given by gavage to mice on day 1, 8 and 15. As a vehicle control, 25 μ l DMSO diluted with 275 μ l PBS was given on the same day.

Histopathological analysis

The dorsal skin was removed 1 day after the final injection. The skin pieces were fixed with 10% formaldehyde for 24 h followed by embedding in paraffin and sectioning using a microtome. Slides were stained with haematoxylin and eosin (H&E). For immunohistochemical analysis, sections were hydrated by passage through xylene and graded ethanols. Next, slides were blocked with 2% bovine serum albumin for 10 min, stained with primary antibody for 60 min (anti-smooth muscle actin 1:50 dilution, DAKO-Cytomation, Carpinteria, CA, USA and mouse monoclonal anti-TACE antibody 1:200 dilution, R&D Systems, Minneapolis, MN, USA). After washing with Tris-Buffered Saline (TBS) containing 0.05% Triton-X100 (TBST), slides were developed using the DAKO ChemMate Envision Kit/HRP (Dako-Cytomation, Carpinteria, CA, USA) followed by counterstaining with haematoxylin. Rabbit IgG was used as the isotype control.

Determination of sTNFRp55, sTNFRp75 and TNF α

Serum samples were obtained from mice before the first injection (day 0) and 1 day after the last injection (day 22). sTNFRp55, sTNFRp75 and TNF α were measured using an enzyme-linked immunosorbent assay (ELISA; R&D Systems). For the *in vitro* assay, mouse primary keratinocytes, mouse primary fibroblasts, mouse splenocytes and C2C12 cells were deprived of serum for 12 h. Variable doses of BLM (100 nM, 1 μ M, 10 μ M) were added and the cell culture supernatants were collected 24 h later for sTNFRp55 analysis.

In situ hybridization

Tissue sections were de-waxed with xylene and rehydrated through an ethanol series and PBS. The sections were fixed with 4% paraformaldehyde in PBS for 15 min and then washed with PBS. For antigen retrieval, the sections were treated with 10 μ g/ml Proteinase K in PBS for 30 min at 37°C. Next, slides were washed with PBS, refixed with 4% paraformaldehyde in PBS, again washed with PBS and placed in 0.2 M HCl for 10 min. After washing with PBS, the sections were acetylated by incubation in 0.1 M triethanolamine-HCl (pH 8.0) with 0.25% acetic anhydride for 10 min. After washing with PBS, the sections were dehydrated through an ethanol series. Hybridization was performed with probes at concentrations of 100 ng/ml in Probe Diluent (Genostaff, Tokyo, Japan) at 60°C for 16 h. After hybridization, the sections were washed in 5x HybriWash (Genostaff) (equal to 5xSSC) at 60°C for 20 min. Subsequently, slides were washed

in 50% formamide (2x HybriWash) at 60°C for 20 min followed by RNase treatment (50 µg/ml RNaseA, 10 mM Tris-HCl, 1 M NaCl, 1 mM ethylenediaminetetraacetic acid (EDTA), pH 8.0) for 30 min at 37°C. The sections were washed twice with 2x HybriWash at 60°C for 20 min, twice with 0.2x HybriWash at 60°C for 20 min and once with TBST (0.1% Tween20 in TBS). After treatment with 0.5% blocking reagent (Roche, Indianapolis, IN, USA) in TBST for 30 min, the sections were incubated with anti-DIG AP conjugate (Roche) diluted to 1:1000 with TBST for 2 h. The sections were washed twice with TBST and then incubated in 100 mM NaCl, 50 mM MgCl₂, 0.1% Tween 20 and 100 mM Tris-HCl pH 9.5. Colouring reactions were performed with BM purple AP substrate (Roche) overnight and followed by washing with PBS. Sections were counterstained with Kernechtrot stain solution (Mutoh, Tokyo, Japan), dehydrated and mounted with Malinol (Mutoh).

RNA isolation and real-time polymerase chain reaction

Sections of skin lesions removed 1 day after the final injection, and cells incubated with variable doses of BLM (100 nM, 1 µM, 10 µM) for 6 and 24 h were collected. Total RNA was isolated using the SV Total RNA Isolation System (Promega, Madison, WI, USA). The product was reverse-transcribed into first-strand complementary DNA (cDNA). Thereafter, the expression of collagen type I $\alpha 1$ (Col1a1) and TGF- $\beta 1$ were measured using the Power SYBR green PCR Master Mix (Applied Biosystems, Foster City, CA, USA) according to the manufacturer's protocol. Glyceraldehyde-3-phosphate dehydrogenase (GAPDH) was used to normalize the mRNA. Sequence-specific primers were designed as follows: Col1a1, sense 5'-gagccctcgctccgtactc-3', antisense 5'-tggtccctactcagcgtctgt-3'; TGF- $\beta 1$, sense 5'-cgaatgtctgacgtattgaagaaca-3', antisense 5'-ggagcccgaagcggacta-3'; GAPDH, sense 5'-tgcctcactctggcagggttct-3', antisense 5'-catggccttccgtgttctca-3'. Real-time PCR (40 cycles of denaturing at 92°C for 15 s and annealing at 60°C for 60 s) was run on an ABI 7000 Prism (Applied Biosystems).

Western blot analysis

Skin samples were frozen in liquid nitrogen, then solubilized at 4°C in lysis buffer (0.5% sodium deoxycholate, 1% Nonidet P40, 0.1% sodium dodecyl sulphate, 100 µg/ml phenylmethylsulphonyl fluoride, 1 mM sodium orthovanadate and protease inhibitor cocktail). Ten micrograms of protein were fractionated on SDS-polyacrylamide gels and transferred onto PVDF membranes (Bio-Rad, Hercules, CA, USA). Non-specific protein binding was blocked by incubating the membranes in 5% w/v non-fat milk powder in TBST (50 mM Tris-HCl, pH 7.6, 150 mM NaCl and 0.1% v/v Tween-20). The membranes were incubated with mouse monoclonal anti-TACE antibody (R&D Systems) at

a dilution of 1:1000 overnight at 4°C or with mouse monoclonal anti- β -actin (Sigma-Aldrich, St Louis, MO, USA) at a dilution of 1:5000 for 30 min at room temperature. After three 5-min washes in TBST, membranes were incubated with Horse radish peroxidase (HRP)-conjugated anti-mouse antibody at a dilution of 1:10 000 for 60 min at room temperature. Protein bands were detected using the ECL Plus kit (GE Healthcare, Buckinghamshire, UK).

Collagen analysis in the sclerotic skin

Six-millimeter skin punch biopsies were homogenized in acetic acid at 4°C to extract collagen. One milligram of pepsin was added to each homogenized sample, which was incubated at 4°C for 24 h with shaking. The pepsin-solubilized material was collected after removal of the insoluble residue by centrifugation at 35 000 g for 60 min at 4°C. The extracted collagen was analysed using 5% polyacrylamide gel electrophoresis, and the gels were stained with Coomassie brilliant blue to identify the pepsin-resistant collagen band.

Statistical analysis

The data are expressed as mean values \pm standard deviation (SD). The unpaired Student's *t*-test was used to determine the level of significance between the sample means.

Results

Serum sTNFRp55 is increased in BLM-treated wild-type mice

Initially, we investigated serum concentration of sTNFRp55 in a murine model of skin fibrosis induced by subcutaneous BLM injection. The BLM-treated group started exhibiting skin sclerosis after 2 weeks of BLM injections, meanwhile the PBS-treated group did not. On day 22, a significant elevation in serum sTNFRp55 was observed in the BLM-treated group. Serum sTNFRp75 also was moderately increased in BLM-treated group (Fig. 1a,b). As TNFRp55 and TNFRp75 are processed by TACE to become soluble, we postulated that BLM might have increased the expression or the activity of TACE. We compared the protein expression of TACE and found higher levels in BLM-treated skin compared with skin from PBS-treated mice (Fig. 1c). Therefore, we next investigated whether the TACE inhibitor, TAPI-1, is able to reduce skin fibrosis induced by BLM injection.

Low dose of TAPI-1 inhibits BLM-induced shedding of TNFRp55 but not TNFRp75

We first examined the effect of TAPI-1 alone. As the inhibitory effect of TAPI-1 depends on its dosage (TNFRp55: IC₅₀ = 5–10 µM, TNFRp75: IC₅₀ = 25–50 µM, TNF α : IC₅₀ = 50–100 µM), we started with a very low-dose TAPI-1 that is supposed to inhibit proteolytic release of sTNFRp55 specifically. Administration of 1 µmol TAPI-1 significantly

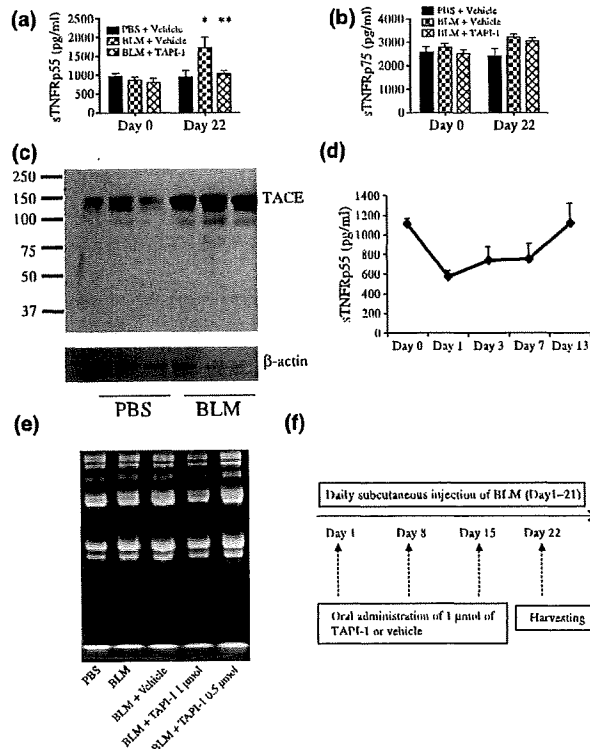


Figure 1. Serum levels of sTNFRp55 and sTNFRp75 in BLM-treated mice. Serum levels of sTNFRp55 (a) and sTNFRp75 (b) were measured by ELISA from mice subcutaneously injected daily with PBS 100 μ l/day, or BLM 1 mg/ml, 100 μ l/day with or without TAPI-1 administration. Three mice in each group were examined. Each histogram shows the mean (\pm SD) of each group. * P < 0.05 versus PBS group, ** P < 0.05 versus BLM group. (c) Typical western blot of TACE in PBS-treated and BLM-treated dorsal skin at day 22. (d) Changes in the serum level of sTNFRp55 after administration of TAPI-1 on day 0. (e) Collagen analysis of sclerotic skin. Collagen was extracted from skin lesions and analysed using 5% polyacrylamide gel electrophoresis. (f) Treatment schedule.

reduced the serum level of sTNFRp55 and was effective for up to 7 days (Fig. 1d). Thus, we decided to administer TAPI-1 weekly in the BLM-induced skin fibrosis model. When administered weekly, 1 μ mol TAPI-1 reduced the amount of collagen in skin lesions although 0.5 μ mol did not (Fig. 1e). From these results, we developed our treatment schedule as shown in Fig. 1f. Wild-type mice received daily subcutaneous injections of PBS or BLM, with or without oral administration of 1 μ mol of TAPI-1 on days 1, 8 and 15. At this dose, TAPI-1 inhibited the release of TNFRp55 (Fig. 1a) but not TNFRp75 (Fig. 1b). TNF α was not detectable (<4.3 pg/ml) during this experiment. From this result, we determined that this dosage and interval of TAPI-1 were optimal to decrease the serum concentration of sTNFRp55 alone.

TAPI-1 inhibits BLM-induced dermal thickening

We next investigated the effect of TAPI-1 on skin thickening. The dorsal skin of the mice was harvested 1 day after the last

BLM injection for histological analysis. As previously reported, BLM-injected skin showed histopathological features such as acanthosis, dermal thickening and adipose tissue atrophy. To our surprise, BLM-injected skins of TAPI-1-administered group were easy to pinch, which indicated improvement of the skin sclerosis. Histological examination also revealed the symptomatic relief from the BLM-induced events. In particular, TAPI-1 significantly inhibited dermal thickening induced by daily BLM injection (Fig. 2a,b). Administration of TAPI-1 alone did not alter skin thickness (P = 0.18, 0.27 ± 0.058 mm in Vehicle + PBS group versus 0.36 ± 0.075 mm in TAPI-1 + PBS group).

Myfibroblasts were decreased in number in the TAPI-1 group

Systemic sclerosis patients' skin is characterized by an increased number of myfibroblasts. These cells are active forms of fibroblasts, which express alpha smooth muscle actin (α -SMA), and are known to contribute to the pathogenesis of SSc (20). To investigate the effect of TAPI-1, the number of myfibroblasts in the skin lesions was counted. As a result, the number of α -SMA-positive cells was significantly increased in the BLM-injected regional skin, while it

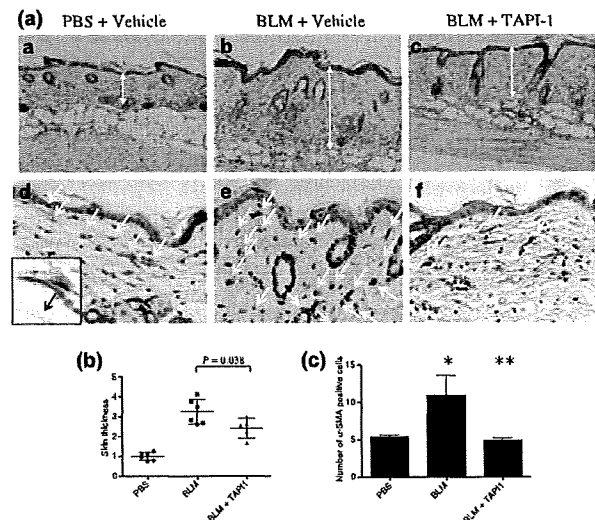


Figure 2. Histological analysis of the skin. (a–c) Haematoxylin and eosin (H&E) staining of PBS + vehicle, BLM + vehicle, BLM + TAPI-1 treated mice skin on day 22 (original magnification $\times 100$), (d–f) immunohistochemistry of α -smooth muscle actin (α -SMA) in myfibroblasts (arrows; original magnification $\times 100$). The small box shows a higher magnification of α -SMA positive cells. (g) Dermal thickness of BLM (n = 6) and BLM + TAPI-1 (n = 5) treated mice compared with PBS (n = 6) treated mice. Two sections from each mouse were evaluated and five locations in each section were measured. The average was calculated and shown as dermal thickness in each mouse. (h) The number of α -SMA-positive cells. * P < 0.01 versus PBS group. ** P < 0.01 versus the BLM group. Horizontal bars represent the mean value and the mean \pm SD of each group.

was decreased in the TAPI-1-administered group (Fig. 2a,c). This result indicates that TAPI-1 might be effective during the early fibrosing phase as the number of myofibroblasts is increased in early lesions of skin sclerosis (21).

Expression of collagen-associated genes

Next, to evaluate the effect of TAPI-1 on the synthesis of collagen and induction of fibrogenic cytokines, RNA extracted from the dorsal skin lesions of mice was analysed for the expression of collagen-associated genes. The expression of *Coll1a1* and the fibrotic cytokine *TGF β 1* were lower in the TAPI-1 group than the BLM group (Fig. 3). These results help to corroborate the efficacy of TAPI-1 in this model.

TACE expression is increased in keratinocytes and muscle fibres in skin tissue

To determine the source of sTNFRp55 in our model, we performed *in situ* hybridization (ISH) and immunohistochemical staining (IHC) for TACE in skin tissue. ISH assay revealed the increased mRNA expression in the epidermis and muscle, which was remarkable in the skin lesions of BLM-treated mice (Fig. 4). In support of this observation, increased TACE protein expression in BLM-induced sclerotic skin also was observed by IHC and western blotting (Figs 1c and 5). To investigate whether BLM directly increased sTNFRp55 in these tissues, we compared the concentration of sTNFRp55 in the supernatant and the expression of the TACE mRNA in the cell lysates of primary mouse keratinocytes, primary mouse fibroblasts and mouse skeletal muscle cell lines (C2C12) after adding BLM *in vitro*. We also added BLM to primary mouse splenocytes *in vitro* because it was recently reported that macrophages are activated in the skin of patients with localized sclero-

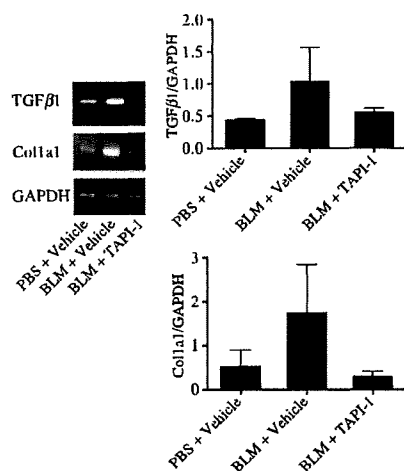


Figure 3. Expression of genes up-regulated in fibrotic tissue. RNA was extracted from the skin lesions. Three mice in each group were investigated. Horizontal bars represent mean values and means \pm SD of each group.

derma (22). We did not observe any increase in the level of sTNFRp55 and TACE in any of these culture cells (data not shown). This finding suggests that the increase of sTNFRp55 in BLM-induced skin fibrosis probably requires multiple cell-cell interactions and some humoral factors.

Discussion

The skin is severely affected by fibrosis in SSc. Although multiple cytokines and other factors are known to contribute to the development of fibrosis, there are no therapeutic approaches that specifically interfere with any of these factors (2). In this study, we focussed on anti-fibrotic signals and targeted TACE, a sheddase of TNFRp55. We showed that oral administration of TAPI-1 significantly inhibited BLM-induced dermal fibrosis.

It was reported by Bohgaki et al. that there was up-regulated expression of TACE in peripheral monocytes of patients with early SSc (23). The expression of TACE protein in monocytes of early-stage SSc patients (disease duration less than 3 years) was significantly higher than in chronic SSc patients and healthy controls. Its expression in SSc patients who received haematopoietic stem cell transplantation (HSCT) was down-regulated 6 months after HSCT. We investigated the expression of TACE in the skin of mice, which was remarkable in the epidermis and muscle, and was increased by BLM injections (Fig. 4). It is interesting that TACE expression is prominent in muscles,

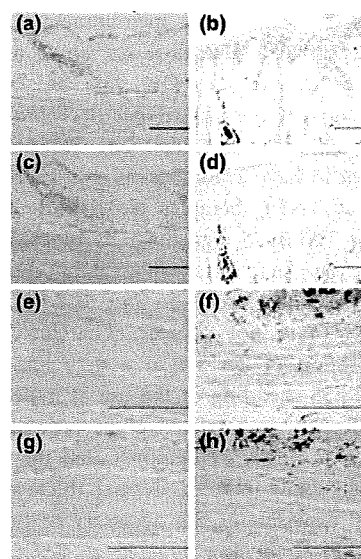


Figure 4. TACE mRNA expression was observed in epidermis and muscle of PBS- and BLM-treated mice by *in situ* hybridization. (Scale bar; 100 μ m) Positive reaction appeared as purple to blue colour, and counterstaining reaction appeared as red colour. (a, b) Epidermis of PBS-treated (a) and BLM-treated (b) mice. (e, f) Muscle of PBS-treated (e) BLM-treated (f) mice. (c, d), (g), (h) are control sense probe of (a), (b), (e), (f).

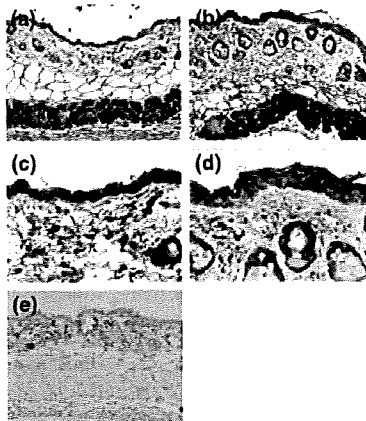


Figure 5. Immunohistochemical staining of the TACE in PBS- and BLM-treated mice. (a) PBS-treated and (b) BLM-treated mice. (original magnification $\times 100$) (c) and (d) are high magnification ($\times 200$) of (a) and (b). (e) Isotype control. $n = 6$ in BLM and PBS group and $n = 5$ in BLM + TAPI-1 group. Representative data are shown.

as fibrosis in SSc patients starts in the deep dermis. Further investigation is needed to show the potential involvement of muscle in skin sclerosis.

It is controversial whether blocking $\text{TNF}\alpha$ in SSc patients is effective or not. Although not well-designed controlled studies, there are some reports that mention the effectiveness of anti- $\text{TNF}\alpha$ therapies in SSc patients (24,25). Recently, it was reported that etanercept was effective in BLM-induced SSc (26). On the contrary, Chizzolini et al. reports that collagen type I production by dermal fibroblasts is inhibited by membrane-associated $\text{TNF}\alpha$, which suggests that $\text{TNF}\alpha$ blockade aimed at controlling fibrosis may be unwise (27). Our data and our previous findings (10) support the importance of $\text{TNF}\alpha/\text{TNFRp55}$ signalling as an anti-fibrotic signal. The $\text{TNF}\alpha/\text{TNFR}$ superfamily is known to have a unique and non-redundant function (20). As anti- $\text{TNF}\alpha$ therapies block both $\text{TNF}\alpha/\text{TNFRp55}$ and $\text{TNF}\alpha/\text{TNFRp75}$ signalling, its blockage may have adverse effects. In fact, intraperitoneal injection of $\text{TNF}\alpha$ did not reduce skin sclerosis in our BLM-induced skin sclerosis model (data not shown). Therefore, we think that the application of TAPI-1 at a very low dose only to block TNFRp55 shedding or the use of molecules that block only TNFRp55 may be effective in treating skin sclerosis.

In this study, we demonstrated that TAPI-1 significantly inhibits BLM-induced dermal thickening. Although additional experiments are necessary to find the site of action of TAPI-1, therapy targeted at TACE may show promise for SSc patients in the future.

Acknowledgements

We thank Professor Junji Takeda at the Department of Social and Environmental Medicine, Graduate School of Medicine, Osaka University, for helpful discussions and Fu Han for technical assistance.

References

- Denton C P, Black C M, Abraham D J. Mechanisms and consequences of fibrosis in systemic sclerosis. *Nat Clin Pract Rheumatol* 2006; **2**: 134–144.
- Steen V. Targeted therapy for systemic sclerosis. *Autoimmun Rev* 2006; **5**: 122–124.
- Trojanowska M, LeRoy E C, Eckes B, Krieg T. Pathogenesis of fibrosis: type I collagen and the skin. *J Mol Med* 1998; **76**: 266–274.
- Uitto J, Kouba D. Cytokine modulation of extracellular matrix gene expression: relevance to fibrotic skin diseases. *J Dermatol Sci* 2000; **24** (Suppl. 1): S60–S69.
- Leask A, Denton C P, Abraham D J. Insights into the molecular mechanism of chronic fibrosis: the role of connective tissue growth factor in scleroderma. *J Invest Dermatol* 2004; **122**: 1–6.
- McGaha T L, Bona C A. Role of profibrogenic cytokines secreted by T cells in fibrotic processes in scleroderma. *Autoimmun Rev* 2002; **1**: 174–181.
- Abraham D J, Shiwen X, Black C M, Sa S, Xu Y, Leask A. Tumor necrosis factor alpha suppresses the induction of connective tissue growth factor by transforming growth factor-beta in normal and scleroderma fibroblasts. *J Biol Chem* 2000; **275**: 15220–15225.
- Yamane K, Ihn H, Asano Y, Jinnin M, Tamaki K. Antagonistic effects of $\text{TNF}\alpha$ on TGF-beta signaling through down-regulation of TGF-beta receptor type II in human dermal fibroblasts. *J Immunol* 2003; **171**: 3855–3862.
- Kahari V M, Chen Y Q, Su M W, Ramirez F, Uitto J. Tumor necrosis factor-alpha and interferon-gamma suppress the activation of human type I collagen gene expression by transforming growth factor-beta 1. Evidence for two distinct mechanisms of inhibition at the transcriptional and posttranscriptional levels. *J Clin Invest* 1990; **86**: 1489–1495.
- Murota H, Hamasaki Y, Nakashima T, Yamamoto K, Katayama I, Matsuyama T. Disruption of tumor necrosis factor receptor p55 impairs collagen turnover in experimentally induced sclerodermic skin fibroblasts. *Arthritis Rheum* 2003; **48**: 1117–1125.
- Hebbar M, Gillot J M, Hachulla E et al. Early expression of E-selectin, tumor necrosis factor alpha, and mast cell infiltration in the salivary glands of patients with systemic sclerosis. *Arthritis Rheum* 1996; **39**: 1161–1165.
- Alecu M, Geleriu L, Coman G, Galatescu L. The interleukin-1, interleukin-2, interleukin-6 and tumour necrosis factor alpha serological levels in localised and systemic sclerosis. *Rom J Intern Med* 1998; **36**: 251–259.
- Heilig B, Fiehn C, Brockhaus M, Gallati H, Pezzutto A, Hunstein W. Evaluation of soluble tumor necrosis factor (TNF) receptors and TNF receptor antibodies in patients with systemic lupus erythematoses, progressive systemic sclerosis, and mixed connective tissue disease. *J Clin Immunol* 1993; **13**: 321–328.
- Gruschwitz M S, Albrecht M, Vieth G, Hausteiner U F. In situ expression and serum levels of tumor necrosis factor-alpha receptors in patients with early stages of systemic sclerosis. *J Rheumatol* 1997; **24**: 1936–1943.
- Majewski S, Wojas-Pelc A, Malejczyk M, Szymanska E, Jablonska S. Serum levels of soluble TNF alpha receptor type I and the severity of systemic sclerosis. *Acta Derm Venereol* 1999; **79**: 207–210.
- Black R A, Rauch C T, Kozlosky C J et al. A metalloproteinase disintegrin that releases tumour-necrosis factor-alpha from cells. *Nature* 1997; **385**: 729–733.
- Newton R C, Solomon K A, Covington M B et al. Biology of TACE inhibition. *Ann Rheum Dis* 2001; **60** (Suppl. 3): iii25–iii32.
- Sano S, Itami S, Takeda K et al. Keratinocyte-specific ablation of Stat3 exhibits impaired skin remodeling, but does not affect skin morphogenesis. *EMBO J* 1999; **18**: 4657–4668.
- Gallucci R M, Sloan D K, Heck J M, Murray A R, O'Dell S J. Interleukin 6 indirectly induces keratinocyte migration. *J Invest Dermatol* 2004; **122**: 764–772.
- Heligans T, Pfeffer K. The intriguing biology of the tumour necrosis factor/tumour necrosis factor receptor superfamily: players, rules and the games. *Immunology* 2005; **115**: 1–20.
- Kissin E Y, Merkel P A, Lafyatis R. Myofibroblasts and hyalinized collagen as markers of skin disease in systemic sclerosis. *Arthritis Rheum* 2006; **54**: 3655–3660.
- Higashi-Kuwata N, Makino T, Inoue Y, Takeya M, Ihn H. Alternatively activated macrophages (M2 macrophages) in the skin of patient with localized scleroderma. *Exp Dermatol* 2009 3 March.
- Bohgaki T, Amasaki Y, Nishimura N et al. Up regulated expression of tumour necrosis factor (alpha) converting enzyme in peripheral monocytes of patients with early systemic sclerosis. *Ann Rheum Dis* 2005; **64**: 1165–1173.
- Tutuncu Z, Morgan G J Jr, Kavanaugh A. Anti-TNF therapy for other inflammatory conditions. *Clin Exp Rheumatol* 2002; **20**: S146–151.
- Alexis A F, Strober B E. Off-label dermatologic uses of anti-TNF-a therapies. *J Cutan Med Surg* 2005; **9**: 296–302.
- Koca S S, Isik A, Ozercan I H, Ustundag B, Evren B, Metin K. Effectiveness of etanercept in bleomycin-induced experimental scleroderma. *Rheumatology (Oxford)* 2008; **47**: 172–175.
- Chizzolini C, Parel Y, De Luca C et al. Systemic sclerosis Th2 cells inhibit collagen production by dermal fibroblasts via membrane-associated tumor necrosis factor alpha. *Arthritis Rheum* 2003; **48**: 2593–2604.

CASE REPORT

Case of schwannomatosis

Yukako MURAKAMI,¹ Mari WATAYA-KANEDA,¹ Mari TANAKA,¹ Akira MYOUI,² Yoshiharu SAKATA,³ Ichiro KATAYAMA¹

Departments of ¹Dermatology and ²Orthopedics, Osaka University School of Medicine, and ³Department of Otorhinolaryngology, Suita City Hospital, Osaka, Japan

ABSTRACT

A 40-year-old man presented to our hospital with painful tumors in his left carotid space and left knee. He had no family history of neurofibromatosis type II (NF II), no history of hearing loss or vestibular problems, and no symptoms of NF I. Magnetic resonance imaging (MRI) of the head revealed no intracranial tumors including vestibular schwannoma (VS). MRI of the left carotid and left knee demonstrated T₁-weighted mass lesions. They were excised and all of them were pathologically diagnosed as schwannoma. Thus, this case was diagnosed as definite schwannomatosis in reference to the diagnostic criteria.

Key words: diagnostic criteria, non-vestibular schwannomas, schwannomatosis.

INTRODUCTION

Schwannomatosis is a recently recognized third major form of neurofibromatosis^{1,2} that causes multiple schwannomas without vestibular tumors. It is sometimes difficult to distinguish schwannomatosis from neurofibromatosis type II (NF II).^{3,4} In 2005, diagnostic criteria for schwannomatosis was defined by MacCollin *et al.*⁵ Some modifications were added by Baser *et al.* in 2006.⁶ We report a case of definite schwannomatosis in reference to the diagnostic criteria.

CASE REPORT

A 40-year-old man was presented to our clinic. He was suffering from painful tumors in his left carotid space and left knee, and another tumor was found on his sacral vertebrae lesion. He had no family history of NF II, and no history of hearing loss or vestibular problems. He had no symptoms of NF I such as café-au-lait spots and neurofibromas. Laboratory findings were all normal. Cranial magnetic resonance imaging

(MRI) revealed no intracranial tumors including vestibular schwannoma (VS). MRI of the sacral vertebrae showed one more mass lesion that was thought to be a schwannoma.

Magnetic resonance imaging of the left carotid (Fig. 1a) and left knee (Fig. 1b) demonstrated T₁-weighted mass lesions. All the T₂-weighted images showed highly intense peripheral rim.

The tumors of the neck and knee were excised and all of them were pathologically examined and diagnosed as schwannomas. They were encapsulated and well circumscribed. The tumors pathologically consisted of two components. Antoni A areas were of a highly ordered cellular component (Fig. 2a). Spindle cells were arranged in short bundles, and showed nuclear palisading, whorling of the cells. Verocay bodies were found in the area. S-100 protein could be demonstrated particularly in Antoni A areas (Fig. 2b). Antoni B areas were far less orderly and less cellular, and had some mucinous changes (Fig. 2c). According to these results, the tumors were pathologically diagnosed as schwannomas.

Correspondence: Mari Wataya-Kaneda, M.D., Ph.D., Department of Dermatology, Osaka University School of Medicine, 2-15 Yamadaoka, Suita-shi, Osaka 565-0871, Japan. Email: mkaneda@derma.med.osaka-u.ac.jp
Received 2 May 2008; accepted 7 May 2009.

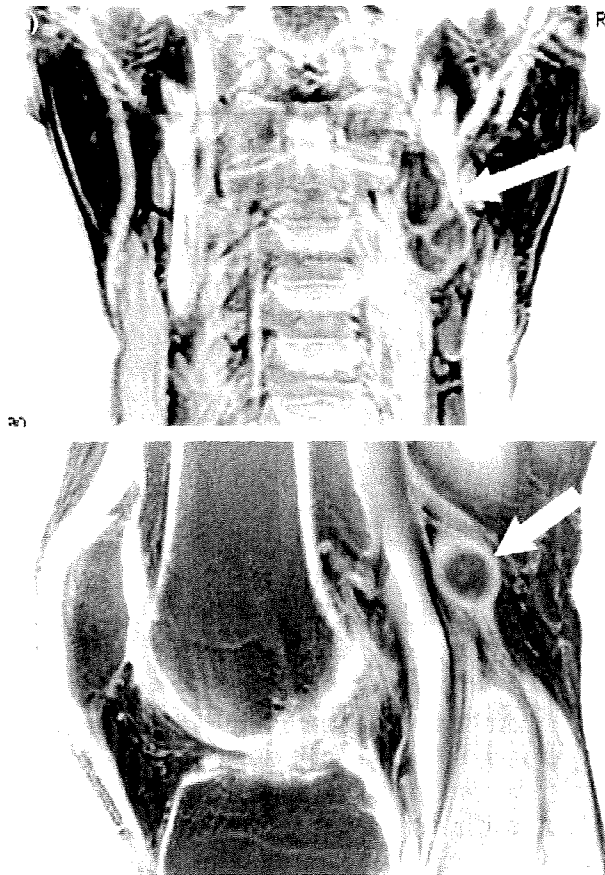


Figure 1. (a) T₁-weighted magnetic resonance image (MRI) of the left carotid space. (b) T₁-weighted MRI of the left knee shows an oval mass continuous to the nerve.

DISCUSSION

Schwannomatosis is an autosomal dominant hereditary disease characterized by multiple schwannomas without VS. The locus of the disease is placed proximal to NF II locus on chromosome 22q.⁷ Although it is a hereditary disease,^{2,7-9} the number of hereditary cases is small⁵ because of low penetrance and incomplete heterogeneity.^{7,9} Thus, schwannomatosis has been recognized as the third major form of NF. Although schwannomatosis and NF II are different diseases, it is quite difficult to distinguish between them from symptoms. However, it is important to distinguish schwannomatosis from NF II, because NF II would be accompanied by hearing loss due to VS. The prognosis of NF II would be worse than that of schwannomatosis.⁵ Pain would be severer in schwannomatosis than in NF II.⁵ In 2005, MacCollin *et al.*

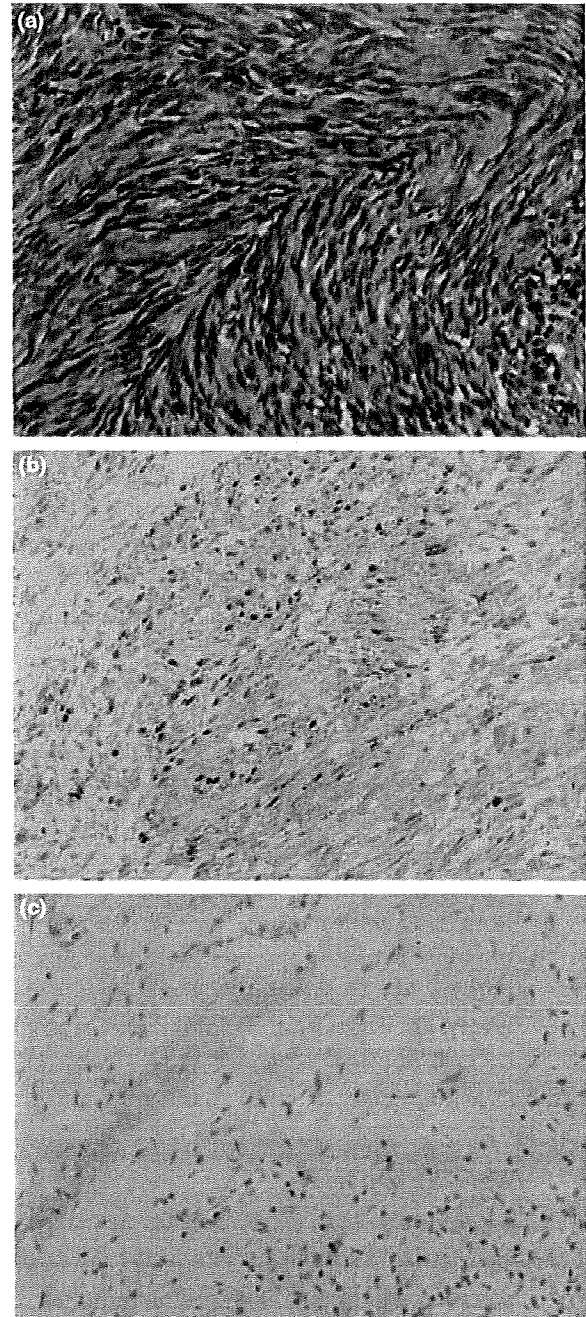
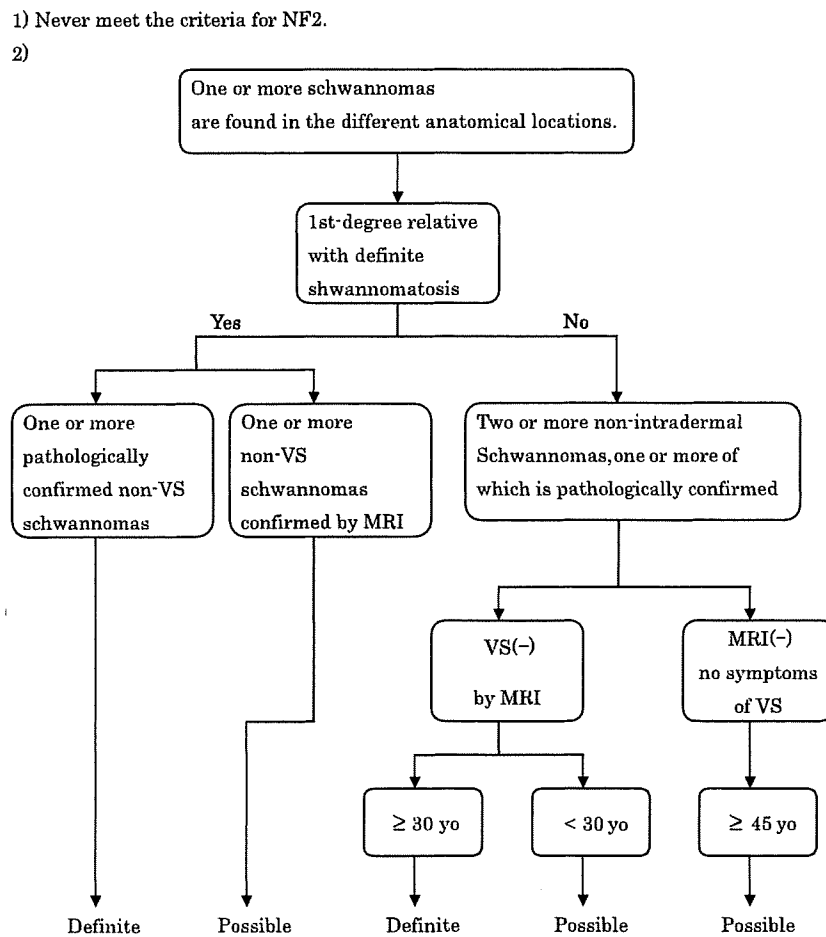


Figure 2. Pathological findings of the tumor mass in the left carotid space. (a) Hematoxylin–eosin (HE) stain in Antoni A areas reveals spindle cells arranged in short bundles with nuclear palisading and Verocay bodies. (b) S-100 protein stain, which can be detected in the cells of the nervous system, can be seen in this schwannoma, particularly in Antoni A areas. (c) Alcian blue stain in Antoni B areas reveal spindle or oval cells arranged haphazardly in the loosely textured matrix. Delicate collagen fibers and irregularly spaced vessels are visible. The mucin is stained blue.

proposed a clinical criteria.⁵ Then, in 2006, Baser *et al.* recommended modifications of diagnostic criteria for schwannomatosis.⁶ We summarized the criteria, and made the following flow chart to apply to our case (Fig. 3). In our case, the patient had non-intradermal schwannomas in the different anatomical locations – left cervical space, left knee and sacral vertebrae – and two of them were pathologically confirmed as schwannomas. He had no first relative with definite schwannomatosis, and had no VS on

MRI. He was over 30 years old. Thus this case was diagnosed as definite schwannomatosis. Many cases of schwannomatosis have been reported in the last 11 years, but many of them did not meet the criteria. In some cases, family history was not referred or the patients were younger than 30 years old.^{1,10-12} In other cases, they had schwannomas in the intradermal tissue. In many cases, all the schwannomas were found in the same anatomical locations.¹³⁻¹⁶ Such cases should be diagnosed as



(This case)

VS; vestibular schwannoma

3) Segmental schwannomatosis is limited to one limb or five or fewer contiguous segments of the spine.

Adapted from the Table by MacCollin on *Neurology* 2005; 64: 1843.

Figure 3. Diagnostic criteria for schwannomatosis. MRI, magnetic resonance imaging; NF, neurofibromatosis; VS, vestibular schwannoma.

segmental schwannomatosis.⁵ Although it had been reported that approximately 2% of the patients with schwannomas are that of schwannomatosis,¹⁷ it should be fewer when we diagnose exactly. Only seven authors have reported 21 non-segmental definite schwannomatosis.^{1,8,9,11,18-20} In Japan, only two authors have reported four non-segmental definite schwannomatosis.^{19,20}

In our case different anatomical lesions were affected. It is important to determine multiple schwannomas strictly. The tumors in the carotid space were thought to be arising from the sympathetic nerve because Horner syndrome appeared after operation, and the tumors of the knee were thought to be arising from the tibial nerve because they were attached to the nerve. Another tumor was also found on his sacral vertebrae lesion. Thus, these tumors were arising from different anatomical spaces, and included the central nervous system.

Here, we reported a case of schwannomatosis that meets the criteria of MacCollin and has schwannomas in the different anatomical locations. This report will be helpful for diagnosis of schwannomatosis, because the disease is rare in Japan.

REFERENCES

- 1 MacCollin M, Woodfin W, Kronn D, Short MP. Schwannomatosis: a clinical and pathologic study. *Neurology* 1996; **46**: 1072-1079.
- 2 Evans DG, Mason S, Huson SM, Ponder M, Harding AE, Strachan T. Spinal and cutaneous schwannomatosis is a variant form of type 2 neurofibromatosis. *J Neurol Neurosurg Psychiatry* 1997; **62**: 361-366.
- 3 Seppala MT, Sainio MA, Haltia MJ, Kinnunen JJ, Setälä KH, Jaaskelainen JE. Multiple schwannomatosis: schwannomatosis or neurofibromatosis type 2? *J Neurosurg* 1998; **89**: 36-41.
- 4 Leverkus M, Kluwe L, Roll EM *et al*. Multiple unilateral schwannomatosis: segmental neurofibromatosis type 2 or schwannomatosis? *Br J Dermatol* 2003; **148**: 804-809.
- 5 MacCollin M, Chiocca EA, Evans DG *et al*. Diagnostic criteria for schwannomatosis. *Neurology* 2005; **64**: 1838-1845.
- 6 Baser ME, Friedman JM, Evans DG. Increasing the specificity of diagnostic criteria for schwannomatosis. *Neurology* 2006; **66**: 730-732.
- 7 MacCollin M, Willett C, Heinrich B *et al*. Familial schwannomatosis: exclusion of the NF2 locus as the germline event. *Neurology* 2003; **60**: 1968-1974.
- 8 Westhout FD, Mathews M, Pare LS, Armstrong WB, Tully P, Linskey ME. Recognizing schwannomatosis and distinguishing it from neurofibromatosis type 1 or 2. *J Spinal Disord Tech* 2007; **20**: 329-332.
- 9 Hulsebos TJ, Plomp AS, Wolterman RA, Robanus-Maandag EC, Baas F, Wesseling P. Germline mutation of INI1/SMARCB1 in familial schwannomatosis. *Am J Hum Genet* 2007; **80**: 805-810.
- 10 Huang J, Mobbs R, Teo C. Multiple schwannomas of the sciatic nerve. *J Clin Neurosci* 2003; **10**: 391-393.
- 11 Huang JH, Simon SL, Nagpal S, Nelson PT, Zager EL. Management of patients with schwannomatosis: report of six cases and review of literature. *Surg Neurol* 2004; **62**: 353-361.
- 12 Kim DH, Hwang JH, Park S-T, Shin JH. Schwannomatosis involving peripheral nerves: a case report. *J Korean Med Sci* 2006; **21**: 1136-1138.
- 13 Katsumi K, Ogose A, Hotta T, Hatono H, Kawashima H, Umezumi H, Endo N. Plexiform schwannoma of the forearm. *Skeletal Radiol* 2003; **32**: 719-723.
- 14 Yamamoto T, Maruyama S, Mizuno K. Schwannomatosis of the sciatic nerve. *Skeletal Radiol* 2001; **30**: 109-113.
- 15 Senchenkov A, Krieger A, Staren ED, Allison DC. Use of intraoperative ultrasound in excision of multiple schwannomas of the thigh. *J Clin Ultrasound* 2005; **33**: 360-363.
- 16 Hasham S, Matteucci P, Stanley PR. Schwannomatosis: multiple schwannomas of upper limb. *J Hand Surg Br* 2006; **31**: 182-184.
- 17 Enzinger FM, Weiss SM. Benign tumors of peripheral nerves. In: Enzinger FM, Weiss SW, eds. *Soft Tissue Tumors*, 4th edn. St Louis, MO: Mosby, 2001; 1146-1171.
- 18 Traistaru R, Enachescu V, Manuc D, Gruia C, Ghilusi M. Multiple right schwannoma. *Rom J Morphol Embryol* 2008; **49**: 235-239.
- 19 Tada K, Miyauchi A, Iwasaki M, Okuda S, Aono H. Clinical results of spinal schwannomatosis. *Chubu-nipponseikeigekasagaigakkaizasshi* 2002; **45**: 895-896.
- 20 Kuroki S, Chosa E, Sakamoto T. Case reports of schwannomatosis in limbs. *Seikeigekatosagaigeka* 2004; **53**: 71-74.